Micro-/nano-plastics accentuate Parkinson's Disease-relevant phenotypes in a *Drosophila* model

Simon A. Lowe[1*] and James E.C. Jepson[1]

[1]Department of Epilepsy, UCL Queen Square Institute of Neurology, London, UK

*To whom correspondence should be addressed: s.lowe@ucl.ac.uk

ABSTRACT

Micro- and nano-plastic (MNP) particles are a ubiquitous environmental contaminant that are increasingly bioaccumulating in human tissues, particularly the brain. MNPs induce mitochondrial defects, oxidative stress, inflammatory responses and neurotoxicity in cellular and organismal models. This raises the possibility that MNP exposure could cause or exacerbate neurological conditions associated with these pathological phenomena. Parkinson's Disease (PD), a common movement disorder characterised by degeneration of striatal dopaminergic neurons, and associated with mitochondrial dysfunction, represents such a condition. We therefore hypothesised that MNP exposure might interact with PD risk mutations affecting mitochondrial fidelity. We used a fruit fly model of *PRKN*-dependent PD associated with defects in mitophagy, a mitochondrial quality control pathway, to test this hypothesis. We found that ingestion of MNPs at concentrations tolerated by wild-type controls selectively enhanced PD-relevant phenotypes – including progressive dopaminergic neurodegeneration, movement defects, and sleep disruption – in this model of PD. Our data suggest that defects in mitochondrial quality control can increase vulnerability to MNP exposure, and more broadly, that MNPs may synergistically interact with existing genetic risk factors to worsen neurological disease.

INTRODUCTION

The rapidly changing environment has the potential to impact human neuronal health via increasing global temperatures [1], reduced air quality [2], and exposure to neurotoxic environmental pollutants [3]. Collectively, neurological disorders are currently the leading cause of disability worldwide; and incidence rates and associated social challenges are expected to increase in the coming decades [4]. Due to the ageing global population, this increase is projected to be particularly prominent for age-related neurological disorders such as Parkinson's Disease (PD) [5]. Thus, understanding how the changing environment may impact the incidence and progression of these disorders is essential to inform policy and shape social responses.

The impact of plastic pollution on human health [6], and particularly neurological health [7] [8], is emerging as a potential global health crisis. Micro- and nano-plastics (MNPs) are defined as plastic particles on the $\leq$ 1 μM and 1 μM - 1 mm scale respectively, which are either manufactured or generated from the breakdown of macro-plastics by UV light degradation, mechanical abrasion from water and sand, etc [9]. Global annual plastic production exceeds 400 million tons, a majority of which are single-use, and only a small minority of which is recycled [10]. MNP pollution is now ubiquitous: significant levels have been identified in the air, soil, ocean and drinking water, including in remote regions [9], with evidence that they bioaccumulate up the food chain [11]. Unsurprisingly given the range of absorption routes, MNPs have been isolated in a range of human tissues [12]. MNPs cross the blood-brain barrier (BBB) and preferentially bioaccumulate in the brain over other tissues [13]. Levels in post-mortem human brain tissue positively correlate with more recent time of death (2016 vs 2024) [12], consistent with increasing environmental levels. Particularly worryingly, MNPs have been identified in the placenta [14], indicating that nervous system exposure to constantly rising MNP levels from the earliest stages of development onwards will now be the norm. The health implications of this exposure are not understood, but MNP levels were higher in brains with documented dementia diagnoses [13], suggesting a possible causative

role and indicating an urgent need to understand how MNPs interact with neural tissue and organismal health.

An extensive body of work demonstrates the cytotoxicity of MNPs to cultured cells. Exposure disrupts the morphology and function of mitochondria [15], possibly by binding directly to complex 1 [16], and induces excess production of reactive oxygen species (ROS), oxidative stress [17], and upregulation of inflammatory markers [18]. These effects overlap with cellular mechanisms known to contribute to a range of neurological disorders, particularly PD, in which the mechanistic contributions of mitochondrial dysfunction, oxidative stress, and chronic inflammation are well documented [19]. Dopaminergic neurons, which selectively degenerate in PD, are particularly vulnerable to mitochondrial toxins [20], and exposure to mitotoxic pesticides may contribute to the aetiology of PD [21] [22]. This raises the possibility that exposure to MNPs could similarly induce PD-like symptoms. Indeed, oral ingestion or inhalation of MNPs cause PD-like motor defects and dopaminergic degeneration [23] [24] [25] in mice, alongside a wide range of behavioural defects in vertebrate and non-vertebrate models [26] [27] [28] [29].

On the basis that vulnerable populations are likely to be first impacted by adverse conditions, we hypothesised that MNP exposure might interact with intrinsic genetic risk for PD. Thus, as environmental contamination levels rise, carriers of risk mutations would be expected to be first impacted, prefiguring effects on the general population. The PINK1/Parkin-mediated mitophagy pathway represents a potential nexus for vulnerability. This pathway performs essential mitochondrial quality control by targeting damaged mitochondria for degradation. PINK1 accumulates on the outer membrane of depolarised mitochondria, recruiting the E3 ubiquitin ligase Parkin, which (poly)ubiquitinates mitochondrial outer membrane proteins, tagging the mitochondria for engulfment by the autophagosome and transport to the lysosome for degradation [30]. A number of the strongest genetic risk factors for PD cluster in genes encoding components of this pathway, including *PINK1, PRKN* and *DJ-1* [31] [32]. It is believed that impaired mitophagy results in an

83 accumulation of defective mitochondria, leading to excessive ROS production, oxidative
84 stress and an inflammatory response, which contribute to dopaminergic neurotoxicity [31].
85 Mitophagy is upregulated in response to mitochondrial toxins such as MPP+ and
86 rotenone, and loss-of-function *PRKN* and *PINK1* mutations causing defective mitophagy
87 increase vulnerability to their neurotoxic effects in patient-derived dopaminergic neuronal
88 culture and *Drosophila* models [33 34 35]. Exposure to MNPs also induces PINK1/Parkin-
89 mediated mitophagy in differentiated dopaminergic neuronal cell culture [36]. We therefore
90 hypothesised that genetic defects in this pathway would increase susceptibility to MNP
91 neurotoxicity.
92 We tested this hypothesis using *Drosophila* as an in vivo model. Due to its relatively
93 short lifespan and an extensive toolkit for genetic manipulation, this species represents a
94 powerful system to interrogate age-dependent neurodegeneration, the role of the highly
95 conserved PINK1/Parkin pathway in PD [37], and genetic variance in resistance to
96 environmental toxins associated with PD [38 39]. LOF of the highly conserved *Drosophila*
97 *PRKN* homologue *parkin* (*park*) causes impaired age-related mitophagy [40] and recapitulates
98 key aspects of PD [41 42]. We found that lifetime exposure MNPs in the form of orally ingested
99 polystyrene micro-spheres accelerated dopaminergic neurodegeneration and exacerbated
100 behavioural phenotypes in *park* LOF flies, at levels tolerated by controls. We conclude that
101 disease-associated mutations can alter susceptibility to MNP neurotoxicity; that
102 environmental MNP pollution may impact the incidence or progression of PD; and that
103 genetic variations in mitophagy may define a group at particular risk from MNP exposure.
104
105

106 **RESULTS**

107 **Ingested MNPs enter the brain and induce a cellular stress response in *Drosophila***

108 We raised and maintained control flies and flies homozygous for the well-characterised *park*[1]
109 LOF mutation on food contaminated with 100 parts-per-million (ppm) 100 nm-diameter
110 polystyrene nanospheres (hereafter "MNP food", compared to "std food"). While not faithfully
111 recapitulating the diversity of plastic polymers present in real-world conditions, several
112 studies have reported the effects of similar feeding protocols [43,44,45], and found only subtle
113 effects on viability and behaviour. Hence, this condition allowed us to test for increased
114 vulnerability to conditions known to be broadly tolerated by flies with intact mitophagy.

115 Initially, we validated the effects of this feeding protocol in control flies. While
116 extensive evidence demonstrates that MNPs cross the blood-brain-barrier in humans and
117 mammalian models [13 46], it has been reported that orally-ingested microspheres fail to
118 permeate the *Drosophila* brain [28]. In contrast, we clearly identified ingested fluorophore-
119 tagged MNPs in the brains of adult flies (Fig. 1A and Supp. Fig. 1). The difference between
120 our own and prior studies is likely due to the smaller size of the MNPs used herein (0.1 vs 1-
121 5 μM [28]), which has been demonstrated to affect efficiency of crossing cell membranes [47].

122 Activation via phosphorylation of the c-Jun N-terminal kinase (JNK) is a primary
123 response to ROS production [48 49]. At 20 d post-eclosure, we observed increased levels of
124 phospho-JNK within the horizontal mushroom body lobes - a neuropil region of the brain
125 which receives dopaminergic input [50] and exhibited robust phosphor-JNK
126 immunofluorescence - in flies raised on MNP food (Fig. 1B), confirming that our protocol
127 replicates the extensively reported finding that MNP exposure induces excess ROS
128 production and oxidative stress in a range of model systems [49 51 52]. We did not quantify
129 volume or spatial distribution of MNPs in the brain, but note that MNP localisation does not
130 appear to overlap with regions of high phospho-JNK (Fig. 1B and Supp. Fig. 1), suggesting a
131 systemic stress response.

132

133 **MNP exposure accelerates degeneration of dopaminergic neurons in *park* mutants**

134 The ~ 130 dopaminergic neurons in the adult *Drosophila* brain are well-characterised and
135 readily visualised by immunostaining against the dopamine precursor tyrosine hydroxylase
136 (TH) (Fig. 2A) [50]. *park* LOF causes selective progressive degeneration of the protocerebral
137 posterior lateral 1 (PPL1) subpopulation, while surrounding populations are spared [42]. PPL1
138 neurons are considered to share homology with dopaminergic neurons of the mammalian
139 substantia nigra pars compacta region [53], which selectively degenerate in PD and appear
140 particularly susceptible to mitochondrial damage and oxidative stress [54]. As expected [42],
141 aged (30 d post-eclosure) but not young (3-5 d) *park*^{1} flies raised on std food exhibited an ~
142 20% reduction in TH^{+} cell bodies within the PPL1 cluster. Notably, this trend was
143 exacerbated by lifetime exposure to MNPs (Fig. 2B,C), with no cell loss observed in two
144 other distinct TH^{+} subpopulations (Supp. Fig. 2). These data suggest that MNP exposure
145 does not cause widespread neurodegeneration, but instead exacerbates specific
146 phenotypes induced by *park* LOF. No loss of neurons in any subpopulation was observed in
147 control flies (Fig. 2B-C, Supp. Fig 2), further supporting the premise that defective Parkin-
148 dependent mitophagy increases susceptibility to MNP neurotoxicity.
149

150 **MNPs exacerbate dysfunctional limb kinematics in *park* mutants**

151 The defining clinical characteristic of PD is progressive decline in motor performance [55],
152 which is recapitulated in *park* LOF mutant flies [56]. Based on the accelerated rate of
153 dopaminergic neurodegeneration, we hypothesised that lifetime MNP exposure would
154 exacerbate motor decline in *park*^{1} flies. We tested gross movement in response to a
155 mechanical stimulus at 3, 10, 20 and 30d post-eclosure, using a video-tracking method: the
156 *Drosophila* ARousal Tracking (DART) system [57 58]. As previously reported across a range of
157 assays [59 60], control flies raised on standard food exhibited an age-dependent decline in
158 motor response. Exposure to MNPs caused a transient *increase* in response in 10 d old
159 controls, consistent with the MNP-induced hyperactivity reported in a range of model
160 systems [61 62 44]. As expected, *park*^{1} flies exhibited significantly decreased responses at all

161 time points tested; however, MNP exposure caused no significant difference at any age
162 (Supp. Fig 3).
163
164 We hypothesised that an MNP-induced exacerbation of movement defects might be
165 masked by an opposing tendency towards hyperactivity, or by a 'floor effect', whereby aged
166 *park*[1] flies moved so little that enhancement of the motor phenotype was not apparent. We
167 therefore turned to a more rigorous analysis of locomotor performance, using the Feature
168 Learning Leg Segmentation and Tracking (FLLIT) system [63 58] to analyse limb kinematics in
169 high-speed videos of freely walking flies (Fig. 3A-B). First, we identified three gait
170 parameters by which *park*[1] flies differed from controls. These are: reduced stride length
171 (displacement), reminiscent of the shuffling gait observed in PD [64]; increased non-linearity of
172 limb movement (derived by normalizing the path moved by a limb during a stride to the
173 distance displaced), indicative of a loss of motor co-ordination; and reduced % of time a limb
174 was moving, indicative of a "plodding gait" with greater pauses between limb movements.
175 Testing at 20 d (since by 30 d *park*[1] flies moved very little), we found that long-term
176 MNP exposure exacerbated the reduced displacement and enhanced non-linearity of
177 movement in *park*[1] flies, with no effect on controls (Fig. 3C). The effect on movement % was
178 more complex. Young *park*[1] exposed to MNPs exhibited an increased movement % relative
179 to those raised on standard food, with controls showing a similar, albeit non-significant, trend
180 ($p = 0.08$). By 20 d, however, MNP-exposed control flies exhibited increased movement %
181 relative to those raised on standard food, while the effect had disappeared in *park*[1] flies
182 (Supp. Fig. 4).
183 We conclude that MNP exposure indeed causes hyperactivity, manifesting here as
184 more rapid limb movements while walking, while simultaneously exacerbating the *park*[1]
185 phenotype of a slower, plodding gait. Thus, *park*[1] flies are affected in a qualitatively different
186 manner to controls; first, hyperactivity becomes apparent after shorter periods of exposure
187 due to their enhanced susceptibility to the neurotoxic effects of MNPs, then by the time

188 hyperactivity manifests in controls, the effect is masked by exacerbation of the opposing
189 phenotype of a reduction in movement %.
190
191 **MNP exposure exacerbates night sleep loss in *park*[1] mutants**
192 Sleep dysfunction is increasingly recognised as a feature of PD, both as a primary symptom
193 affecting quality of life, and as a predictor of and potential factor contributing to disease
194 progression [65]. In *Drosophila*, *park* LOF causes circadian abnormalities and sleep
195 disturbance [66 67]. We interrogated the effect of MNP exposure on this phenotype using 5H
196 *Drosophila A*ctivity *M*onitors (DAM5H) (Fig. 4A), a multi-infrared beam system that facilitates
197 high-resolution measures of sleep and activity in *Drosophila* [68]. While we clearly saw an
198 effect of *park*[1] on both day and night sleep (Fig. 4A), we focused on the previously published
199 phenotype of reduced night sleep [66]. Strikingly, in *park*[1] flies, MNP exposure caused a further
200 reduction in night sleep levels by 20 d, with no significant effect observed in control flies (Fig.
201 4A, B).
202 Collectively, the above data demonstrate a detrimental and genotype-specific impact
203 of chronic MNP on disease-relevant phenotypes in a well-characterized *Drosophila* model of
204 PD.
205
206

207 **DISCUSSION**

208

209 MNP pollution is now ubiquitous in the environment, and bioaccumulation in the human
210 brain, together with a wealth of evidence of cytotoxic effects from *in vitro* and *in vivo* models,
211 raise the possibility that chronic exposure could cause or contribute to neurological disease [6]
212 [7]. Understanding how this environmental factor interacts with underlying genetic
213 vulnerabilities can therefore help delineate the scale of the problem and identify populations
214 at specific risk.

215 Together, the data presented herein demonstrate that chronic MNP exposure
216 exacerbates degenerative, motor, and non-motor PD-like phenotypes in an established
217 invertebrate model of *PRKN*-linked PD. We conclude that disease-associated mutations can
218 modify susceptibility to the neurotoxic effects of MNP exposure, that genetic defects in
219 mitophagy may define a subpopulation at particular risk, and that research into MNP
220 pollution as an environmental factor potentially impacting rising rates of PD [5] is warranted.

221 Here, we focused on PD, on the basis that the potential of environmental factors to
222 contribute to PD-like phenotypes is well-established [3 69]; that mitotoxic effects of MNP
223 exposure [15] overlap with the mechanism of action of pesticides associated with PD-like
224 phenotypes [22 70]; and that chronic exposure has been reported to induce dopaminergic
225 neurodegeneration in model systems [23 24 25]. However, the effects of MNP exposure – such
226 as mitochondrial dysfunction, oxidative stress and neuroinflammation [15] – overlap with a
227 cellular mechanisms contributing to a range of neurodegenerative and neurodevelopmental
228 disorders [71 72 73]. Thus, the contribution of plastic pollution to a much wider range of
229 neurological health outcomes should be considered.

230 Here we focused on PD-associated defects in PINK1/Parkin-dependent mitophagy
231 as a genetic risk factor. However, the cellular effects of MNP exposure are widespread, and
232 a large number of mutations affecting a range of cellular processes increase risk for PD [74],
233 so genetic defects in mitophagy are likely not to be unique in increasing susceptibility to
234 MNP exposure is unclear. Further, our interpretation that *park*[1] flies' increased vulnerability

235 to MNPs is due to defective mitophagy is based on extensive published data on the effects
236 of MNP exposure [15], Parkin LOF [40], and the interaction between Parkin LOF and exposure to
237 mitochondrial toxicants [35 75], but is not explicitly demonstrated here. Further work could
238 directly interrogate the molecular mechanisms underlying the interaction between Parkin
239 LOF and MNP toxicity by directly measuring rates of mitophagy, ROS production and
240 accumulation of abnormal mitochondria, and/or strengthen the genetic evidence associating
241 mitophagy with resistance to MNP neurotoxicity by testing whether LOF of other components
242 of the PINK1/Parkin-dependent mitophagy pathway similarly increased vulnerability to MNP
243 exposure [37 32]. Furthermore, while we demonstrate that MNPs permeated the brain, we did
244 not interrogate the extent to which neuronal effects were attributable to MNPs within the
245 brain versus elsewhere in the body, for example via the gut-brain axis [76 45]. These limitations
246 can be addressed through further studies that build upon the data presented in this work.
247 MNPs levels are difficult to assess, due to challenges in direct measurement [77] huge
248 range of particle size and type, geographical differences, and changes over time [78 79 80],
249 leading to a large range of estimates in levels in relevant sources of absorption [81]. The
250 concentrations used in this study are likely to be significantly higher than those most of the
251 global population are currently exposed to. In other ways, however, this feeding protocol
252 may underestimate toxicity; it does not recapitulate the full range of MNP absorption routes
253 [82], particle sizes [47] and shapes [83], or potentially additive interactions with other environmental
254 contaminants [84] present in real-world conditions. Further, since MNPs bioaccumulate in brain
255 tissue over time [13], short-lived organisms such as *Drosophila* may be expected to tolerate
256 higher levels of pollutions than humans. Thus, while we demonstrate a clear interaction
257 between a PD genetic risk factor and exposure to MNPs, further work is required to
258 interrogate the effects in more ecologically relevant conditions.
259
260
261

262 **MATERIALS AND METHODS**

263 **Experimental models and MNP exposure conditions**

264 Experimental models were fruit flies of the species *Drosophila melanogaster*. Flies were
265 maintained on standard fly food under 12 h: 12 h light-dark cycles (12L: 12D) at a constant
266 25°C. Experiments were conducted at the age indicated, on male flies. Genotypes used
267 were *park*[1] (Bloomington *Drosophila* Stock Centre stock number 34747) and the isogenised
268 w^{1118} control line iso[31] (a kind gift from Prof. Kyunghee Koh, Thomas Jefferson University).
269 Flies were raised on a standard food medium. MNP food was generated by mixing 0.1 µM-
270 diameter Opti-Bind polystyrene microparticles (ThermoFisher) to a concentration of 100pp
271 into melted fly food. For visualisation, fluorophore-tagged 0.1 µM-diameter polystyrene
272 FluoSpheres (excitation/emission 540/560) (ThermoFisher) were substituted.

273

274 **Immuno-histochemistry**

275 Brains were dissected in phosphate-buffered saline (PBS) (Sigma Aldrich) at the time point
276 indicated and immuno-stained as described previously [85]. Briefly, brains were fixed by
277 20 min room temperature incubation in 4% paraformaldehyde (MP biomedicals) and blocked
278 for 1 h in 5% normal goat serum in PBS + 0.3% Triton-X (Sigma-Aldrich) (PBT). Brains were
279 incubated overnight in primary antibody at 4°C, washed three times in PBT and incubated
280 overnight in secondary antibody at 4°C, then washed a final time before mounting in
281 SlowFade Gold anti-fade mountant (ThermoFisher). Primary antibodies were rabbit anti-
282 TH/tyrosine hydroxylase (Abcam, ab128249; 1:500) and rabbit anti-phospho-JNK1/JNK2
283 (Thr183, Tyr185) (ThermoFisher MA5-14943; 1:500). Secondary antibody was goat anti-
284 mouse AlexaFluor 647 at 1:1000 (ThermoFisher). Images were taken with a Zeiss LSM 980
285 confocal microscope with an EC 'Plan-Neofluar' 20x/0.50 M27 air objective, taking z-stacks
286 through the entire brain with step sizes of 1-2 µm. Images were visualised and analysed
287 using ImageJ. TH+ cells were manually counted. For fluorescence quantification, z-stacks of
288 the whole brain were 3D-projected using a maximum intensity projection. From these whole-
289 brain stacks, ROIs were drawn around the horizontal mushroom body lobes, an

290 axonal/synaptic neuropil region receiving dopaminergic input. Mean fluorescence values
291 were taken with background subtracted. Brains compared were dissected, stained and
292 imaged in parallel.
293
294 **Locomotor and sleep analysis**
295 DAM:
296 Sleep analysis was performed using the *Drosophila* Activity Monitor 5 system (DAM5H,
297 Trikinetics inc., MA, USA), which improves on the fidelity of the earlier DAM2 system by
298 using 15 infrared beams per tube, rather than a single one, to track movement [68]. Male flies
299 of the age indicated were loaded into glass behavioural tubes (Trikinetics inc., MA, USA)
300 containing 4% sucrose and 2% agar and left for two full days to acclimatise. On the third day
301 the number of beam breaks was measured using *Drosophila* Activity Monitor. Sleep was
302 defined using the standard definition of ≥5 min of inactivity, which has been shown to
303 correlate with postural changes, increased arousal threshold and altered brain activity
304 patterns [68]. Sleep bout number and duration were analysed using the open-source software
305 suite phaseR (https://github.com/abhilashlakshman/phaseR/tree/main) [86].
306
307 DART:
308 As above, flies were loaded into behavioural tubes with flies. After 24 h acclimatisation, a
309 single stimulus in the form of a mechanical vibration (a train of five 200 ms pulses separated
310 by 800 ms intervals, set at the DART system's maximum intensity) was delivered at
311 Zeitgeber Time (ZT) 3. Locomotor activity was recorded using the *Drosophila* ARousal
312 Tracking (DART) system (BFKlabs) [57] as previously described [58]. Videos were taken using a
313 USB webcam (Logitech) and speed (mm / s) was analysed by the DART system from
314 absolute position, and binned in 1 min intervals. Flies were excluded from analysis if they
315 exceeded an average of 1 mm / s speed in the five 1 min bins preceding the stimulus. The
316 mean speed (mm / s) in the 1 min bin following the stimulus was analysed.
317

318 FLLIT:

319 For FLLIT (Feature Learning-based LImb segmentation and Tracking) measurements, de-
320 winged male flies were loaded into custom-made 2x2 cm arenas without anaesthesia. 500
321 fps videos consisting of flies walking in a straight line and taking at least three clear strides
322 were taken using a Photron FASTCAM Mini UX50 High Speed Camera with a Sigma
323 105 mm Macro lens. Gait analysis was performed using the FLLIT system [63], as previously
324 described [58]. Where FLLIT generates data for parameters per stride, the first and last stride
325 were excluded and a mean of the remaining values taken. Values for each leg were pooled,
326 giving six values per fly. Definitions of the parameters used are as follows. *Stride length*:
327 Straight-line distance between the posterior and anterior extreme positions of the limb in
328 each stride. Directly output by FLLIT as "Displacement". *Path / displacement*: Path Travelled
329 (directly output by FLLIT) is the total actual distance covered by a limb during a stride; this is
330 divided by Stride Displacement to compensate for differences in stride length. Larger values
331 indicate greater deviation from an optimal straight-line path. *Movement %*: % of the video for
332 which a given limb is in motion.

333

334 **Quantification and statistical analysis**

335 Statistical analyses were performed using Graphpad Prism. Data sets were tested for normal
336 distributions using the Shapiro-Wilk test. Normally distributed data sets were tested for
337 statistical differences using unpaired t-tests with Welch's correction for non-identical
338 variance, and non-normally distributed data sets were tested using Mann-Whitney U-test.
339 Interactions between genotype and age/food type were analysed using 2-way ANOVA with
340 Sidak's correction for multiple comparisons.

341

ACKNOWLEDGEMENTS

This study was funded by a MRC Senior Non-Clinical Fellowship (MR/V03118X/1) to J.E.C.J, a BBSRC Project Grant (BB/X00094X/1) to S.L and J.E.C.J.

AUTHOR CONTRIBUTIONS

S.A.L – Conceptualization, Methodology, Investigation, Writing - Original Draft, Writing – Review & Editing, Visualization, Funding acquisition; J.E.C.J – Writing – Review & Editing, Supervision, Project administration, Funding acquisition.

DECLARATION OF INTERESTS

The authors declare no competing interests.

355 **FIGURE LEGENDS**

356

357 **Figure 1. Orally ingested polystyrene microspheres permeate the brain and activate**
358 **the JNK stress pathway**

359 **A**. Representative image of a whole ex vivo brain from a 20 d post-eclosure control fly raised
360 on food contaminated with 100ppm fluorophore (540/560)-tagged 0.1 μM polystyrene
361 microspheres. *Left:* tagged micro-spheres; *Centre*: DAPI counterstain; *Right*: merge. Scale
362 bar = 50 μM.

363 **B**. **i.** Representative image of a whole ex vivo brain stained with anti-phospho-JNK, from a
364 20 d post-eclosure control fly raised on (*left*) standard food or (*right*) food contaminated with
365 100ppm 0.1 μM polystyrene microspheres (MNP). Representative ROI around horizontal
366 mushroom body (MB) lobes is indicated. Scale bar = 50 μM. **ii.** Quantified anti-phospho-JNK
367 immunofluorescence within horizontal (MB) lobes (two analysed per brain). Comparison is
368 Mann-Whitney test, *P $\leq$ 0.05.

369

370 **Figure 2. Chronic MNP exposure accelerates degeneration of dopaminergic PPL1**
371 **neurons in *park*^{1} mutants, at dosages tolerated by controls**

372 **A.** *(Top)* Schematic showing the position of the protocerebral posterior medial (PPM) 1-3
373 and protocerebral posterior lateral (PPL) 1-2c clusters of TH^{+} neurons in the adult *Drosophila*
374 brain, with the degenerating PPL1 cluster highlighted. *(Bottom)* Representative ex vivo brain
375 (control, std food, 3 d) immunostained with anti-TH (red) against F-actin counterstain (grey).
376 Scale bar = 50 μm.

377 **B.** Manually counted TH^{+} cell bodies within the PPL1 subpopulation. Grey bars indicate
378 control and blue bars *park*^{1} flies. Empty bars indicate flies raised and maintained on std food;
379 filled bars indicate MNP-containing food. Comparison is 2-way ANOVA, within genotype,
380 with age (young = 3-5 d; aged = 30 d) and diet (std vs MNP-containing food) as factors. *P
381 $\leq$, * 0.05, **P < 0.01

382 **C.** Representative control and *park*[1] ex vivo brains immunostained with anti-TH, comparing
383 young (3-5 d) vs aged (30 d) flies, raised on std vs MNP-containing food. Enlarged insets
384 show left PPL1 subpopulation. Scale bars = 50 μm (main), 25 μm (insets).
385
386 **Figure 3. Chronic MNP exposure exacerbates dysfunctional limb kinematics in *park*[1]**
387 **mutants, at dosages tolerated by controls**
388 **A.** Schematic showing the function of the Feature Learning-based Limb segmentation and
389 Tracking (FLLIT) system for analysing limb kinematics.
390 **B.** Representative FLLIT-derived schematics showing overlaid movement of each limb over
391 multiple strides, relative to body center, for control (left) and *park*[1] 3 d old flies.
392 **C.** Quantification of two FLLIT-derived gait parameters: stride length (displacement) and
393 path/displacement. Data points represent individual limbs, 6 per fly. Comparisons are 2-way
394 ANOVA, within age point, with genotype and diet as factors. *P < 0.05, **P < 0.01, *** P <
395 0.001, ****P < 0.0001.
396
397 **Figure 4. Chronic MNP exposure exacerbates night sleep loss in *park*[1] mutants, at**
398 **dosages tolerated by controls**
399 **A.** *(Left)* Schematic showing function of the DAM5 system. *(Right)* Mean sleep in 12L: 12D
400 conditions of young (5-7 d) and aged (20 d) *park*[1] and control flies, raised on standard or
401 MNP food.
402 **B.** Night sleep, as the fraction of time from ZT12-24 (lights-off) spent asleep. Data points
403 represent individual flies. Comparisons are 2-way ANOVA, within age point, with genotype
404 and diet as factors. *P < 0.05, *** P < 0.001, ****P < 0.0001.
405
406
407
408

409 **SUPPLEMENTARY FIGURE LEGENDS**

410

411 **Supplementary Fig. 1.**

412 Two representative whole ex vivo brains of 20 d post-eclosure control flies raised on food
413 contaminated with 100ppm fluorophore (540/560)-tagged 0.1 μM polystyrene microspheres.
414 Arrows indicate accumulations of MNPs. Scale bar = 50 μM. Note: left image is also shown
415 in Fig. 1A.

416

417 **Supplementary Fig. 2.**

418 **A-B.** Manually counted TH^+ cell bodies within the PPLM1+2 (**A**) and PPM3 (**B**)
419 subpopulations. Grey bars indicate control and blue bars *park*[1] flies. Empty bars indicate
420 flies were raised and maintained on std food; filled bars indicate MNP-containing food.
421 Comparisons are 2-way ANOVA, within genotype, with age (young = 3-5 d; aged = 30 d) and
422 diet (std vs MNP-containing food) as factors. *P < 0.05.

423

424 **Supplementary Fig. 3.**

425 **A.** Schematic showing the use of the *Drosophila* ARousal Tracking (DART) system to assay
426 stimulus-dependent locomotion.

427 **B.** Traces showing average speed (mm / s) over time in 1 min bins for control and *park*[1] 10 d
428 old flies, in standard vs MNP food, in response to a mechanical stimulus occurring at 10
429 mins.

430 **C.** Age-dependent change in motor performance. Quantification of mean speed in the 1 min
431 bin immediately following mechanical stimulus, at 4 age points. *N* values indicated on graph,
432 referring to number of animals. Comparisons are 2-way ANOVA, within genotype, with age
433 (3, 10, 20 and 30d post-eclosure) and diet (std vs MNP-containing food) as factors. **P <
434 0.01.

435

436 **Supplementary Fig. 4.**

Quantification of the FLLIT-derived gait parameter movement %. Data points represent individual limbs, 6 per fly. Comparisons are 2-way ANOVA, within age point, with genotype and diet as factors. *P < 0.05, **P < 0.01, *** P < 0.001, ****P < 0.0001.

442 **REFERENCES**

443 1. Sisodiya, S. M. *et al.* Climate change and disorders of the nervous system. *The Lancet Neurology*
444 **23**, 636–648 (2024).
445 2. Hooper, L. G. & Kaufman, J. D. Ambient Air Pollution and Clinical Implications for Susceptible
446 Populations. *Ann Am Thorac Soc* **15**, S64–S68 (2018).
447 3. Atterling Brolin, K. *et al.* Environmental Risk Factors for Parkinson's Disease: A Critical Review
448 and Policy Implications. *Movement Disorders* **40**, 204–221 (2025).
449 4. Feigin, V. L. *et al.* The global burden of neurological disorders: translating evidence into policy.
450 *Lancet Neurol* **19**, 255–265 (2020).
451 5. Su, D. *et al.* Projections for prevalence of Parkinson's disease and its driving factors in 195
452 countries and territories to 2050: modelling study of Global Burden of Disease Study 2021. *BMJ*
453 **388**, e080952 (2025).
454 6. Landrigan, P. J. *et al.* The Lancet Countdown on health and plastics. *The Lancet* **0**, (2025).
455 7. Zheng, Y., Xu, S., Liu, J. & Liu, Z. The effects of micro- and nanoplastics on the central nervous
456 system: A new threat to humanity? *Toxicology* **504**, 153799 (2024).
457 8. Gao, H.-T. *et al.* From exposure to neurotoxicity induced by micro-nanoplastics with brain
458 accumulation and cognitive decline. *Ecotoxicology and Environmental Safety* **304**, 119114
459 (2025).
460 9. Wang, C., Zhao, J. & Xing, B. Environmental source, fate, and toxicity of microplastics. *Journal of*
461 *Hazardous Materials* **407**, 124357 (2021).
462 10. Houssini, K., Li, J. & Tan, Q. Complexities of the global plastics supply chain revealed in a trade-
463 linked material flow analysis. *Commun Earth Environ* **6**, 257 (2025).
464 11. Saeedi, M. How microplastics interact with food chain: a short overview of fate and impacts. *J*
465 *Food Sci Technol* **61**, 1–11 (2023).
466 12. Roslan, N. S. *et al.* Detection of microplastics in human tissues and organs: A scoping review. *J*
467 *Glob Health* **14**, 04179.

468 13. Nihart, A. J. *et al.* Bioaccumulation of microplastics in decedent human brains. *Nat Med* 1–6
469 (2025) doi:10.1038/s41591-024-03453-1.
470 14. Ragusa, A. *et al.* Plasticenta: First evidence of microplastics in human placenta. *Environ Int* **146**,
471 106274 (2021).
472 15. Lee, S. E., Yi, Y., Moon, S., Yoon, H. & Park, Y. S. Impact of Micro- and Nanoplastics on
473 Mitochondria. *Metabolites* **12**, 897 (2022).
474 16. Huang, Y. *et al.* Polystyrene nanoplastic exposure induces excessive mitophagy by activating
475 AMPK/ULK1 pathway in differentiated SH-SY5Y cells and dopaminergic neurons in vivo. *Particle*
476 *and Fibre Toxicology* **20**, 44 (2023).
477 17. Das, A. The emerging role of microplastics in systemic toxicity: Involvement of reactive oxygen
478 species (ROS). *Science of The Total Environment* **895**, 165076 (2023).
479 18. Gautam, R. *et al.* Evaluation of potential toxicity of polyethylene microplastics on human derived
480 cell lines. *Sci Total Environ* **838**, 156089 (2022).
481 19. Beal, M. F. Mitochondria, oxidative damage, and inflammation in Parkinson's disease. *Ann N Y*
482 *Acad Sci* **991**, 120–131 (2003).
483 20. Wimalasena, K. The inherent high vulnerability of dopaminergic neurons toward mitochondrial
484 toxins may contribute to the etiology of Parkinson's disease. *Neural Regen Res* **11**, 246–247
485 (2016).
486 21. Lüth, T. *et al.* Longitudinal assessment of the association between pesticide exposure and
487 lifestyle with Parkinson's disease motor severity. *NPJ Parkinsons Dis* **11**, 164 (2025).
488 22. Utyasheva, L., Amarasinghe, P. & Eddleston, M. Paraquat at 63—the story of a controversial
489 herbicide and its regulations: It is time to put people and public health first when regulating
490 paraquat. *BMC Public Health* **25**, 3089 (2025).
491 23. Polystyrene nanoplastics trigger pyroptosis in dopaminergic neurons through TSC2/TFEB-
492 mediated disruption of autophagosome-lysosome fusion in Parkinson's disease | Journal of

493 Translational Medicine | Full Text. https://translational-
494 medicine.biomedcentral.com/articles/10.1186/s12967-025-06634-9.
495 24. Liang, B. *et al.* Brain single-nucleus transcriptomics highlights that polystyrene nanoplastics
496 potentially induce Parkinson's disease-like neurodegeneration by causing energy metabolism
497 disorders in mice. *Journal of Hazardous Materials* **430**, 128459 (2022).
498 25. Jeong, H. *et al.* Nanoplastics Cause an Increased Risk of Parkinson's Disease Compared to
499 Microplastics at Environmental Exposure Levels. *Journal of Hazardous Materials Advances*
500 100941 (2025) doi:10.1016/j.hazadv.2025.100941.
501 26. Wang, G., Lin, Y. & Shen, H. Exposure to Polystyrene Microplastics Promotes the Progression of
502 Cognitive Impairment in Alzheimer's Disease: Association with Induction of Microglial
503 Pyroptosis. *Mol Neurobiol* **61**, 900–907 (2024).
504 27. Gaspar, L., Bartman, S., Coppotelli, G. & Ross, J. M. Acute Exposure to Microplastics Induced
505 Changes in Behavior and Inflammation in Young and Old Mice. *Int J Mol Sci* **24**, 12308 (2023).
506 28. Yan, W. *et al.* Microplastic exposure disturbs sleep structure, reduces lifespan, and decreases
507 ovary size in *Drosophila melanogaster*. *zr* **45**, 805–820 (2024).
508 29. Kong, F., Jin, H., Xu, Y. & Shen, J. Behavioral toxicological tracking analysis of *Drosophila* larvae
509 exposed to polystyrene microplastics based on machine learning. *Journal of Environmental*
510 *Management* **359**, 120975 (2024).
511 30. Ashrafi, G. & Schwarz, T. L. The pathways of mitophagy for quality control and clearance of
512 mitochondria. *Cell Death Differ* **20**, 31–42 (2013).
513 31. Pickrell, A. M. & Youle, R. J. The Roles of PINK1, Parkin and Mitochondrial Fidelity in Parkinson's
514 Disease. *Neuron* **85**, 257–273 (2015).
515 32. Imberechts, D. *et al.* DJ-1 is an essential downstream mediator in PINK1/parkin-dependent
516 mitophagy. *Brain* **145**, 4368–4384 (2022).
517 33. Chung, S. Y. *et al.* Parkin and PINK1 Patient iPSC-Derived Midbrain Dopamine Neurons Exhibit
518 Mitochondrial Dysfunction and α-Synuclein Accumulation. *Stem Cell Reports* **7**, 664–677 (2016).

519 34. Schwartzentruber, A. *et al.* Oxidative switch drives mitophagy defects in dopaminergic parkin
520 mutant patient neurons. *Sci Rep* **10**, 15485 (2020).
521 35. Wang, C. *et al.* Drosophila Overexpressing Parkin R275W Mutant Exhibits Dopaminergic Neuron
522 Degeneration and Mitochondrial Abnormalities. *J Neurosci* **27**, 8563–8570 (2007).
523 36. Liu, T., Hou, B., Wang, Z. & Yang, Y. Polystyrene microplastics induce mitochondrial damage in
524 mouse GC-2 cells. *Ecotoxicology and Environmental Safety* **237**, 113520 (2022).
525 37. Clark, I. E. *et al.* Drosophila pink1 is required for mitochondrial function and interacts genetically
526 with parkin. *Nature* **441**, 1162–1166 (2006).
527 38. Villalobos-Cantor, S., Arreola-Bustos, A. & Martin, I. Genetic basis of maneb-induced
528 dopaminergic neurodegeneration in Drosophila. *G3 Genes|Genomes|Genetics* **15**, jkaf159
529 (2025).
530 39. Villalobos-Cantor, S., Arreola-Bustos, A. & Martin, I. Genome-wide analysis reveals genes
531 mediating resistance to paraquat neurodegeneration in Drosophila. *Genetics* **230**, iyaf087
532 (2025).
533 40. Cornelissen, T. *et al.* Deficiency of parkin and PINK1 impairs age-dependent mitophagy in
534 Drosophila. *eLife* **7**, e35878 (2018).
535 41. Cackovic, J. *et al.* Vulnerable Parkin Loss-of-Function Drosophila Dopaminergic Neurons Have
536 Advanced Mitochondrial Aging, Mitochondrial Network Loss and Transiently Reduced
537 Autophagosome Recruitment. *Front. Cell. Neurosci.* **12**, (2018).
538 42. Whitworth, A. J. *et al.* Increased glutathione S-transferase activity rescues dopaminergic neuron
539 loss in a Drosophila model of Parkinson's disease. *Proceedings of the National Academy of*
540 *Sciences* **102**, 8024–8029 (2005).
541 43. Aloisi, M. *et al.* Plastic Fly: What Drosophila melanogaster Can Tell Us about the Biological
542 Effects and the Carcinogenic Potential of Nanopolystyrene. *Int J Mol Sci* **25**, 7965 (2024).
543 44. Matthews, S. *et al.* Polystyrene micro- and nanoplastics affect locomotion and daily activity of
544 Drosophila melanogaster. *Environ. Sci.: Nano* **8**, 110–121 (2021).

545 45. Zhang, Y., Wolosker, M. B., Zhao, Y., Ren, H. & Lemos, B. Exposure to microplastics cause gut
546 damage, locomotor dysfunction, epigenetic silencing, and aggravate cadmium (Cd) toxicity in
547 *Drosophila*. *Science of The Total Environment* **744**, 140979 (2020).
548 46. Shan, S., Zhang, Y., Zhao, H., Zeng, T. & Zhao, X. Polystyrene nanoplastics penetrate across the
549 blood-brain barrier and induce activation of microglia in the brain of mice. *Chemosphere* **298**,
550 134261 (2022).
551 47. Choi, H. *et al.* Size-Dependent Internalization of Microplastics and Nanoplastics Using In Vitro
552 Model of the Human Intestine—Contribution of Each Cell in the Tri-Culture Models.
553 *Nanomaterials (Basel)* **14**, 1435 (2024).
554 48. Ugbode, C. *et al.* JNK signalling regulates antioxidant responses in neurons. *Redox Biol* **37**,
555 101712 (2020).
556 49. Zhang, Y. & Chen, F. Reactive Oxygen Species (ROS), Troublemakers between Nuclear Factor-κB
557 (NF-κB) and c-Jun NH2-terminal Kinase (JNK). *Cancer Res* **64**, 1902–1905 (2004).
558 50. Mao, Z. & Davis, R. L. Eight Different Types of Dopaminergic Neurons Innervate the Drosophila
559 Mushroom Body Neuropil: Anatomical and Physiological Heterogeneity. *Front Neural Circuits* **3**,
560 5 (2009).
561 51. Qiao, R. *et al.* Microplastics induce intestinal inflammation, oxidative stress, and disorders of
562 metabolome and microbiome in zebrafish. *Science of The Total Environment* **662**, 246–253
563 (2019).
564 52. Chen, Y. *et al.* Polystyrene nanoplastics exposure induces cognitive impairment in mice via
565 induction of oxidative stress and ERK/MAPK-mediated neuronal cuproptosis. *Part Fibre Toxicol*
566 **22**, 13 (2025).
567 53. Strausfeld, N. J. & Hirth, F. Deep Homology of Arthropod Central Complex and Vertebrate Basal
568 Ganglia. *Science* **340**, 157–161 (2013).

569 54. Ni, A. & Ernst, C. Evidence That Substantia Nigra Pars Compacta Dopaminergic Neurons Are
570 Selectively Vulnerable to Oxidative Stress Because They Are Highly Metabolically Active. *Front.*
571 *Cell. Neurosci.* **16**, (2022).
572 55. Armstrong, M. J. & Okun, M. S. Diagnosis and Treatment of Parkinson Disease: A Review. *JAMA*
573 **323**, 548–560 (2020).
574 56. Greene, J. C. *et al.* Mitochondrial pathology and apoptotic muscle degeneration in Drosophila
575 parkin mutants. *Proceedings of the National Academy of Sciences* **100**, 4078–4083 (2003).
576 57. Faville, R., Kottler, B., Goodhill, G. J., Shaw, P. J. & van Swinderen, B. How deeply does your
577 mutant sleep? Probing arousal to better understand sleep defects in Drosophila. *Sci Rep* **5**, 8454
578 (2015).
579 58. Lowe, S. A. *et al.* Modulation of a critical period for motor development in Drosophila by BK
580 potassium channels. *Current Biology* **34**, 3488-3505.e3 (2024).
581 59. Iliadi, K. G. & Boulianne, G. L. Age-related behavioral changes in Drosophila. *Annals of the New*
582 *York Academy of Sciences* **1197**, 9–18 (2010).
583 60. Lowe, S. A., Usowicz, M. M. & Hodge, J. J. L. Neuronal overexpression of Alzheimer's disease and
584 Down's syndrome associated DYRK1A/minibrain gene alters motor decline, neurodegeneration
585 and synaptic plasticity in Drosophila. *Neurobiology of Disease* **125**, 107–114 (2019).
586 61. Chen, Q. *et al.* Microplastics Lead to Hyperactive Swimming Behaviour in Adult Zebrafish. *Aquat*
587 *Toxicol* **224**, 105521 (2020).
588 62. Vignon, A. N. *et al.* Lifelong exposure to polystyrene-nanoplastics induces an attention-deficit
589 hyperactivity disorder-like phenotype and impairs brain aging in mice. *Journal of Hazardous*
590 *Materials* **494**, 138640 (2025).
591 63. Banerjee, A., Wu, S., Cheng, L. & Aw, S. S. Fully Automated Leg Tracking in Freely Moving Insects
592 using Feature Learning Leg Segmentation and Tracking (FLLIT). *J Vis Exp*
593 https://doi.org/10.3791/61012 (2020) doi:10.3791/61012.

594 64. Creaby, M. W. & Cole, M. H. Gait characteristics and falls in Parkinson's disease: A systematic
595 review and meta-analysis. *Parkinsonism & Related Disorders* **57**, 1–8 (2018).
596 65. Stefani, A. & Högl, B. Sleep in Parkinson's disease. *Neuropsychopharmacol.* **45**, 121–128 (2020).
597 66. Doktór, B., Damulewicz, M. & Pyza, E. Effects of MUL1 and PARKIN on the circadian clock, brain
598 and behaviour in Drosophila Parkinson's disease models. *BMC Neuroscience* **20**, 24 (2019).
599 67. Julienne, H., Buhl, E., Leslie, D. S. & Hodge, J. J. L. Drosophila PINK1 and parkin loss-of-function
600 mutants display a range of non-motor Parkinson's disease phenotypes. *Neurobiol Dis* **104**, 15–23
601 (2017).
602 68. Sitaraman, D., Vecsey, C. G. & Koochagian, C. Activity Monitoring for Analysis of Sleep in
603 Drosophila melanogaster. *Cold Spring Harb Protoc* **2024**, pdb.top108095 (2024).
604 69. Dorsey, E. R. & Bloem, B. R. Parkinson's Disease Is Predominantly an Environmental Disease. *J*
605 *Parkinsons Dis* **14**, 451–465.
606 70. Uversky, V. N. Neurotoxicant-induced animal models of Parkinson's disease: understanding the
607 role of rotenone, maneb and paraquat in neurodegeneration. *Cell Tissue Res* **318**, 225–241
608 (2004).
609 71. Qin, P., Sun, Y. & Li, L. Mitochondrial dysfunction in chronic neuroinflammatory diseases
610 (Review). *Int J Mol Med* **53**, 47 (2024).
611 72. Chen, Y., Zhou, Z. & Min, W. Mitochondria, Oxidative Stress and Innate Immunity. *Front. Physiol.*
612 **9**, (2018).
613 73. Dash, U. C. *et al.* Oxidative stress and inflammation in the pathogenesis of neurological
614 disorders: Mechanisms and implications. *Acta Pharmaceutica Sinica B*
615 https://doi.org/10.1016/j.apsb.2024.10.004 (2024) doi:10.1016/j.apsb.2024.10.004.
616 74. Nalls, M. A. *et al.* Identification of novel risk loci, causal insights, and heritable risk for
617 Parkinson's disease: a meta-analysis of genome-wide association studies. *The Lancet Neurology*
618 **18**, 1091–1102 (2019).

619 75. Pesah, Y. *et al.* Drosophila parkin mutants have decreased mass and cell size and increased
620 sensitivity to oxygen radical stress. *Development* **131**, 2183–2194 (2004).
621 76. Sofield, C. E., Anderton, R. S. & Gorecki, A. M. Mind over Microplastics: Exploring Microplastic-
622 Induced Gut Disruption and Gut-Brain-Axis Consequences. *Curr Issues Mol Biol* **46**, 4186–4202
623 (2024).
624 77. A. Monikh, F. *et al.* Challenges in studying microplastics in human brain. *Nat Med* 1–2 (2025)
625 doi:10.1038/s41591-025-04045-3.
626 78. Gimiliani, G. T. & Izar, G. Difficulties in Comparison Among Different Microplastic Studies: The
627 Inconsistency of Results and Lack of Guide Values. *Environmental Toxicology and Chemistry* **41**,
628 820–821 (2022).
629 79. Lamichhane, G. *et al.* Microplastics in environment: global concern, challenges, and controlling
630 measures. *Int. J. Environ. Sci. Technol.* **20**, 4673–4694 (2023).
631 80. Zhao, X. & You, F. Microplastic Human Dietary Uptake from 1990 to 2018 Grew across 109 Major
632 Developing and Industrialized Countries but Can Be Halved by Plastic Debris Removal. *Environ.*
633 *Sci. Technol.* **58**, 8709–8723 (2024).
634 81. Mason, S. A., Welch, V. G. & Neratko, J. Synthetic Polymer Contamination in Bottled Water.
635 *Front Chem* **6**, 407 (2018).
636 82. Enyoh, C. E. *et al.* Microplastics Exposure Routes and Toxicity Studies to Ecosystems: An
637 Overview. *Environ Anal Health Toxicol* **35**, e2020004 (2020).
638 83. Martin, L. M. A., Gan, N., Wang, E., Merrill, M. & Xu, W. Materials, Surfaces, and Interfacial
639 Phenomena in Nanoplastics Toxicology Research. *Environ Pollut* **292**, 118442 (2022).
640 84. Yu, F. *et al.* Interaction of microplastics with perfluoroalkyl and polyfluoroalkyl substances in
641 water: A review of the fate, mechanisms and toxicity. *Science of The Total Environment* **948**,
642 175000 (2024).

643 85. Deneubourg, C. *et al.* Epg5 links proteotoxic stress due to defective autophagic clearance and
644 epileptogenesis in Drosophila and Vici syndrome patients. *Autophagy* 1–13 (2024)
645 doi:10.1080/15548627.2024.2405956.
646 86. Persons, J. L. *et al.* PHASE: An Open-Source Program for the Analysis of DrosophilaPhase,
647 Activity, and Sleep Under Entrainment. *J Biol Rhythms* **37**, 455–467 (2022).
648

Figure 1

A

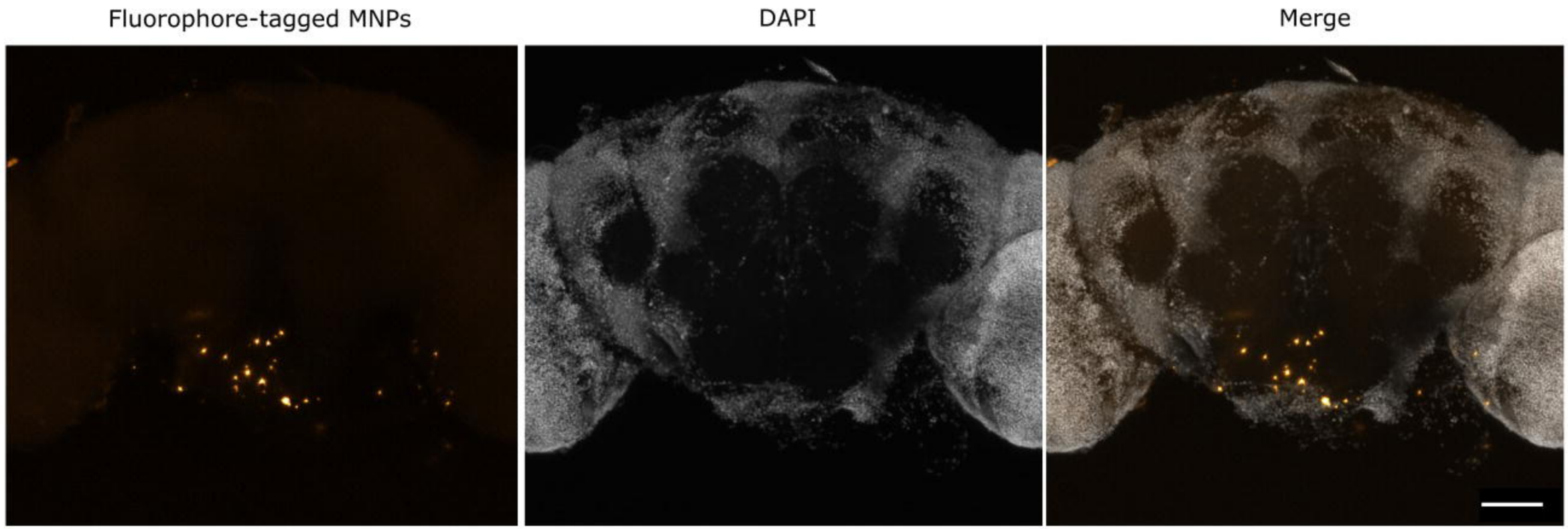

Bi

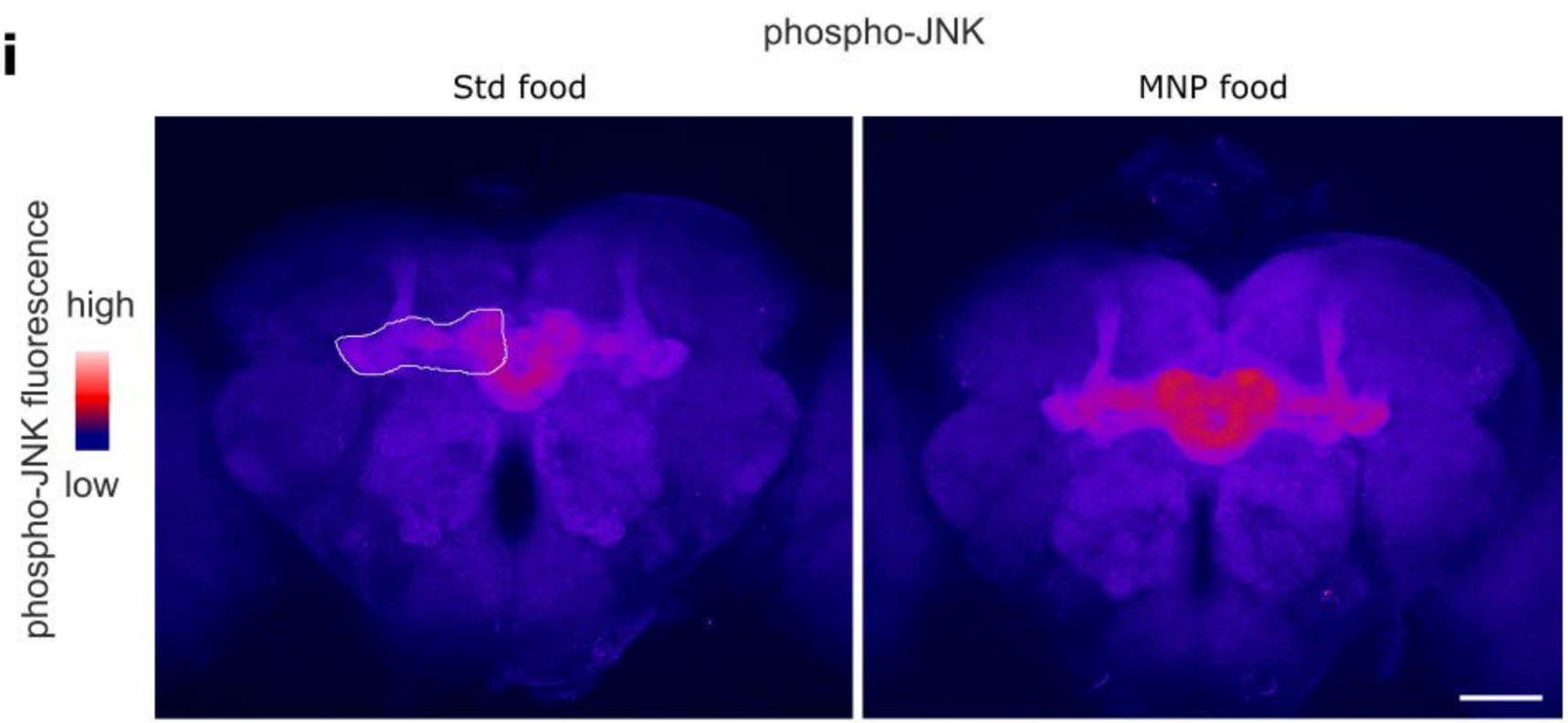

Bii

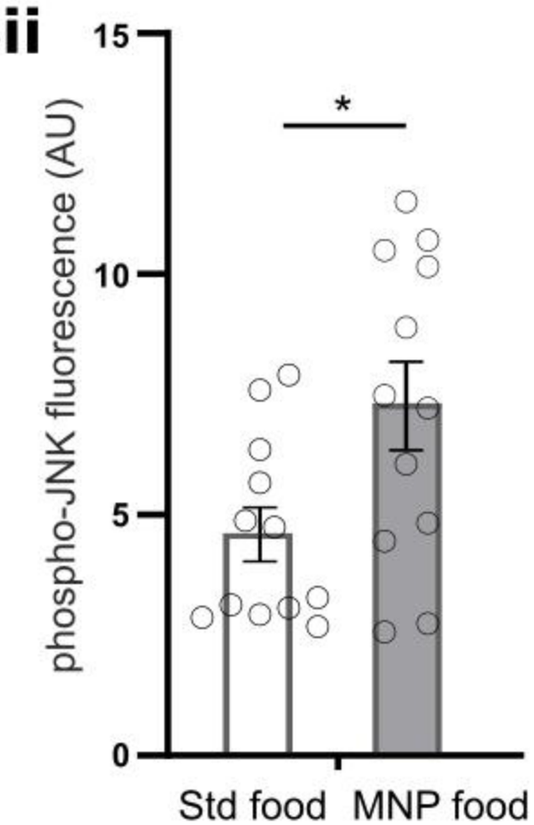

Figure 2

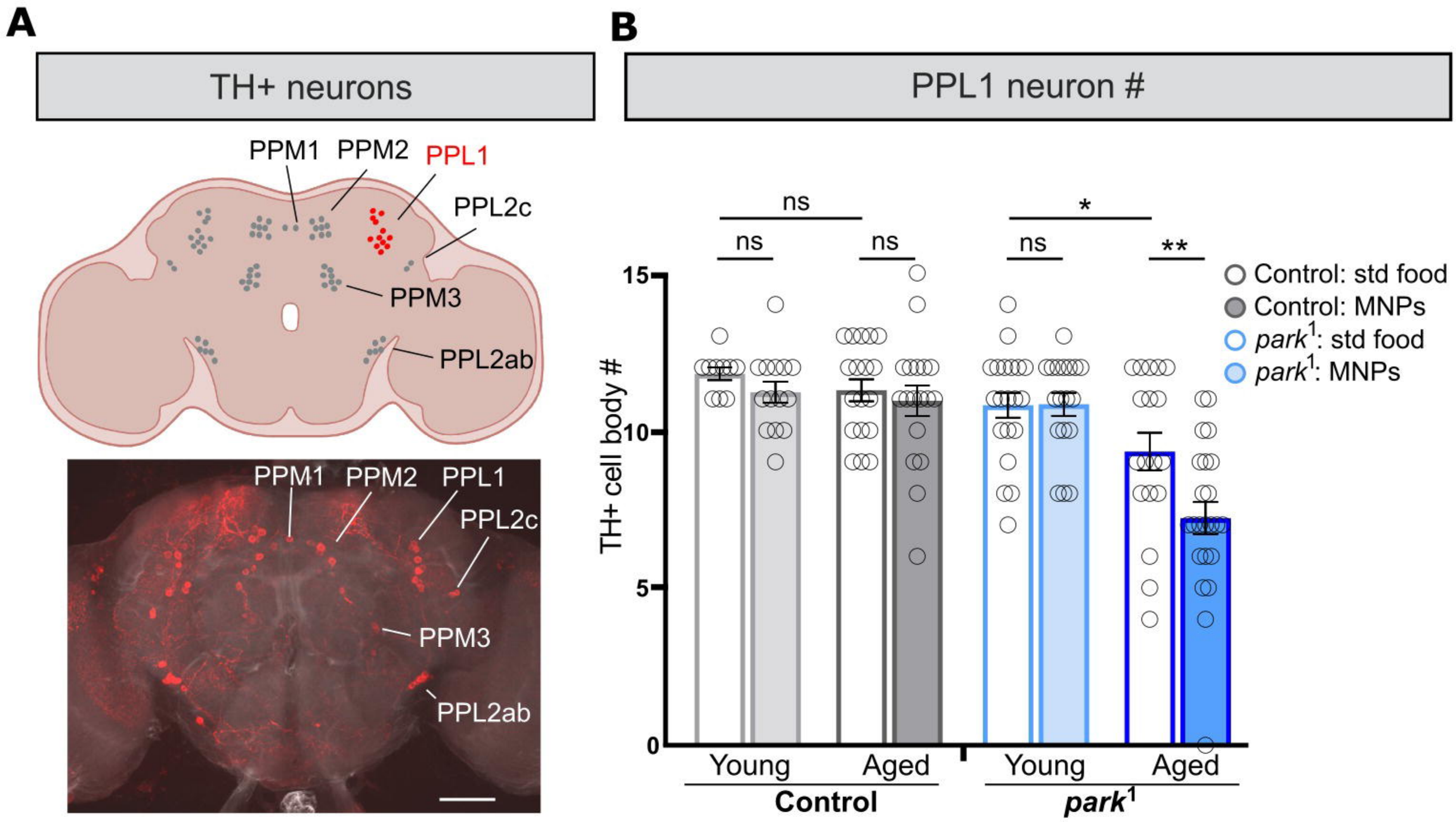
A
TH+ neurons
PPM1
PPM2
PPL1
PPL2c
PPM3
PPL2ab
B
PPL1 neuron #
ns
ns
ns
*
ns
**
TH+ cell body #
15
10
5
0
Control: std food
Control: MNPs
park1: std food
park1: MNPs
Young
Aged
Young
Aged
Control
park1

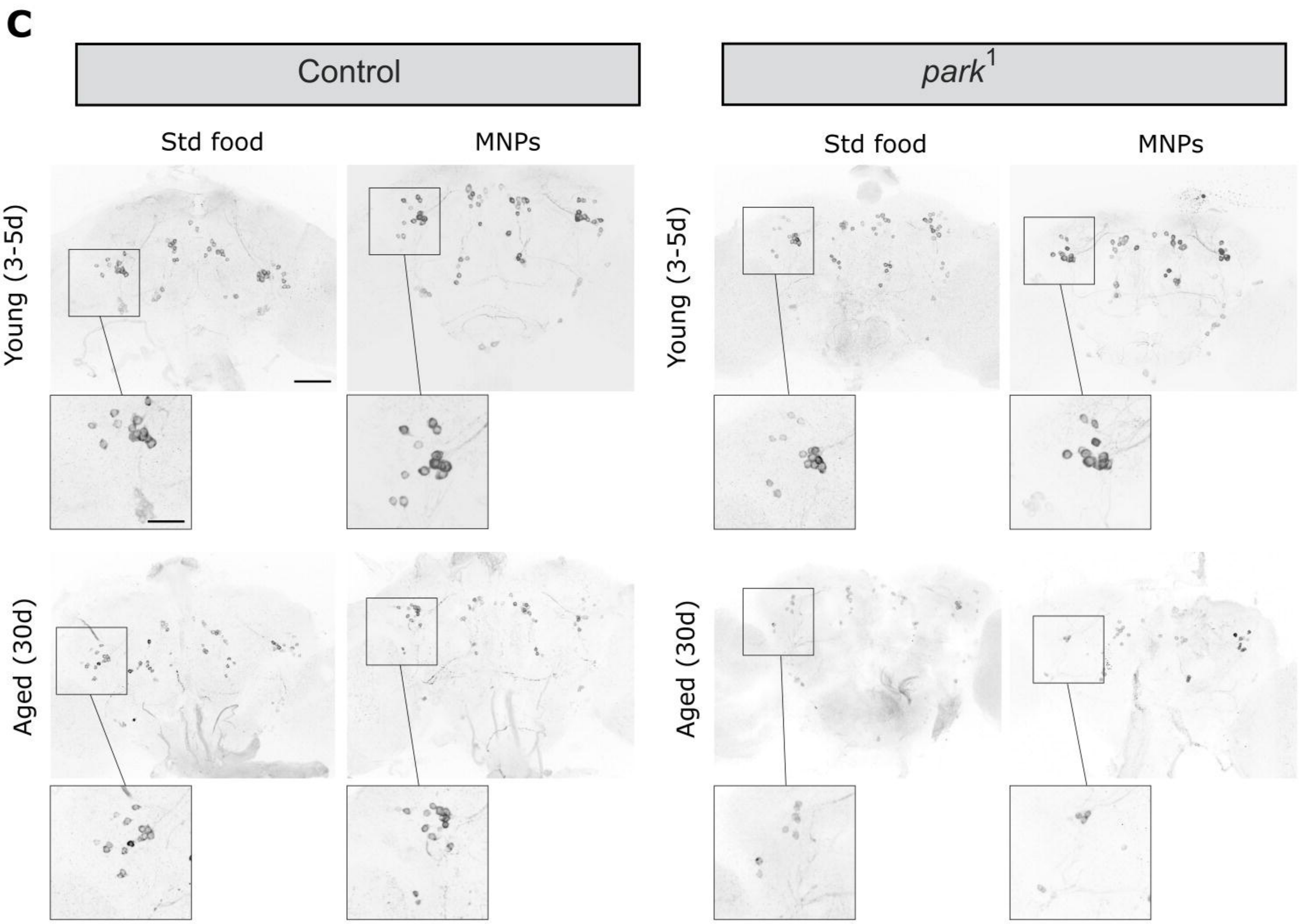
C
Control
park1
Std food
MNPs
Std food
MNPs
Young (3-5d)
Young (3-5d)
Aged (30d)
Aged (30d)

Figure 3

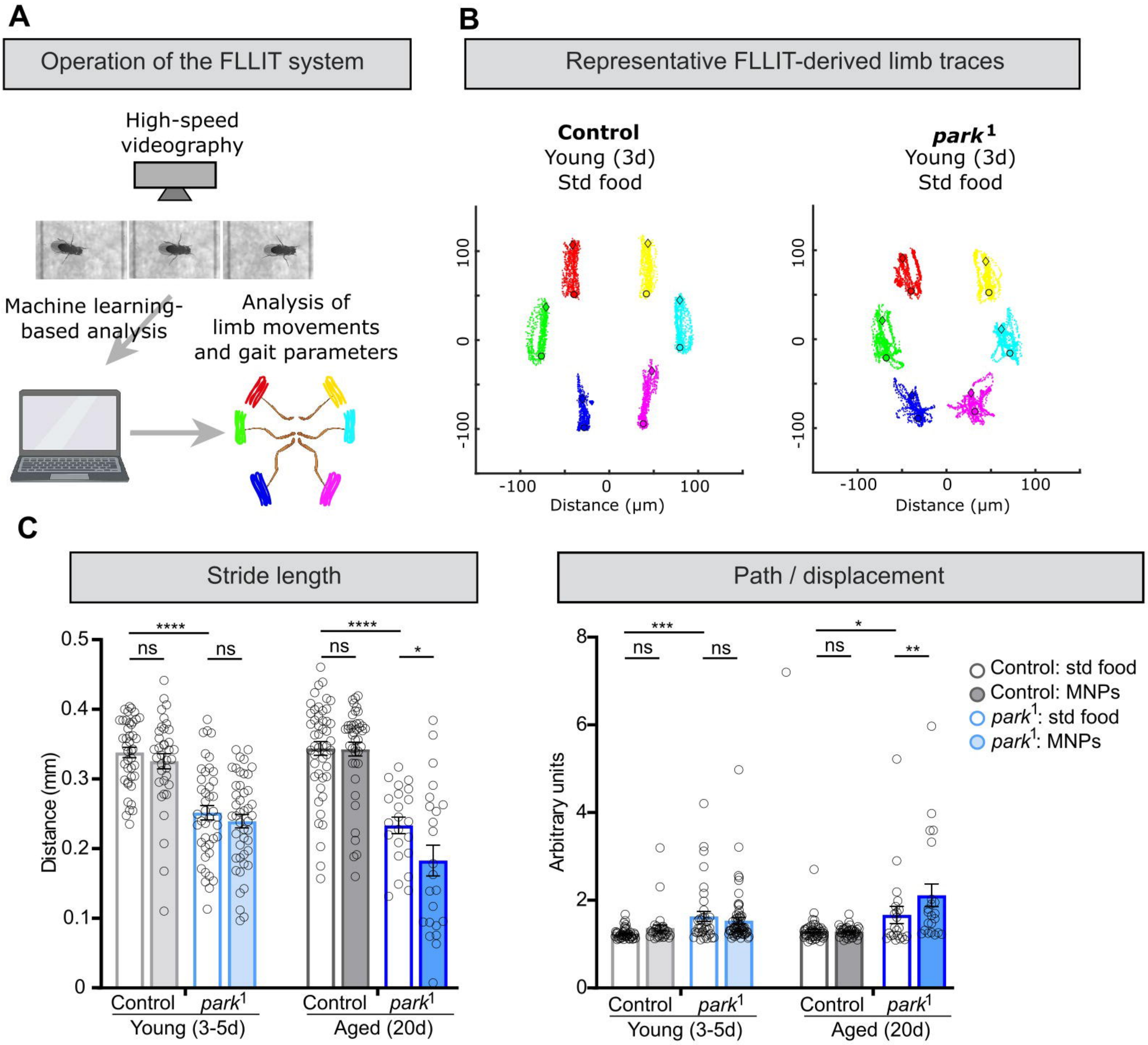
A
Operation of the FLLIT system
High-speed videography
Machine learning-based analysis
Analysis of limb movements and gait parameters
B
Representative FLLIT-derived limb traces
Control
Young (3d)
Std food
park1
Young (3d)
Std food
100
0
-100
-100
0
100
Distance (μm)
C
Stride length
Distance (mm)
0.5
0.4
0.3
0.2
0.1
0
****
ns
ns
****
ns
*
Control
park1
Young (3-5d)
Control
park1
Aged (20d)
Path / displacement
Arbitrary units
8
6
4
2
0
***
ns
ns
*
ns
**
Control
park1
Young (3-5d)
Control
park1
Aged (20d)
Control: std food
Control: MNPs
park1: std food
park1: MNPs

Figure 4

A

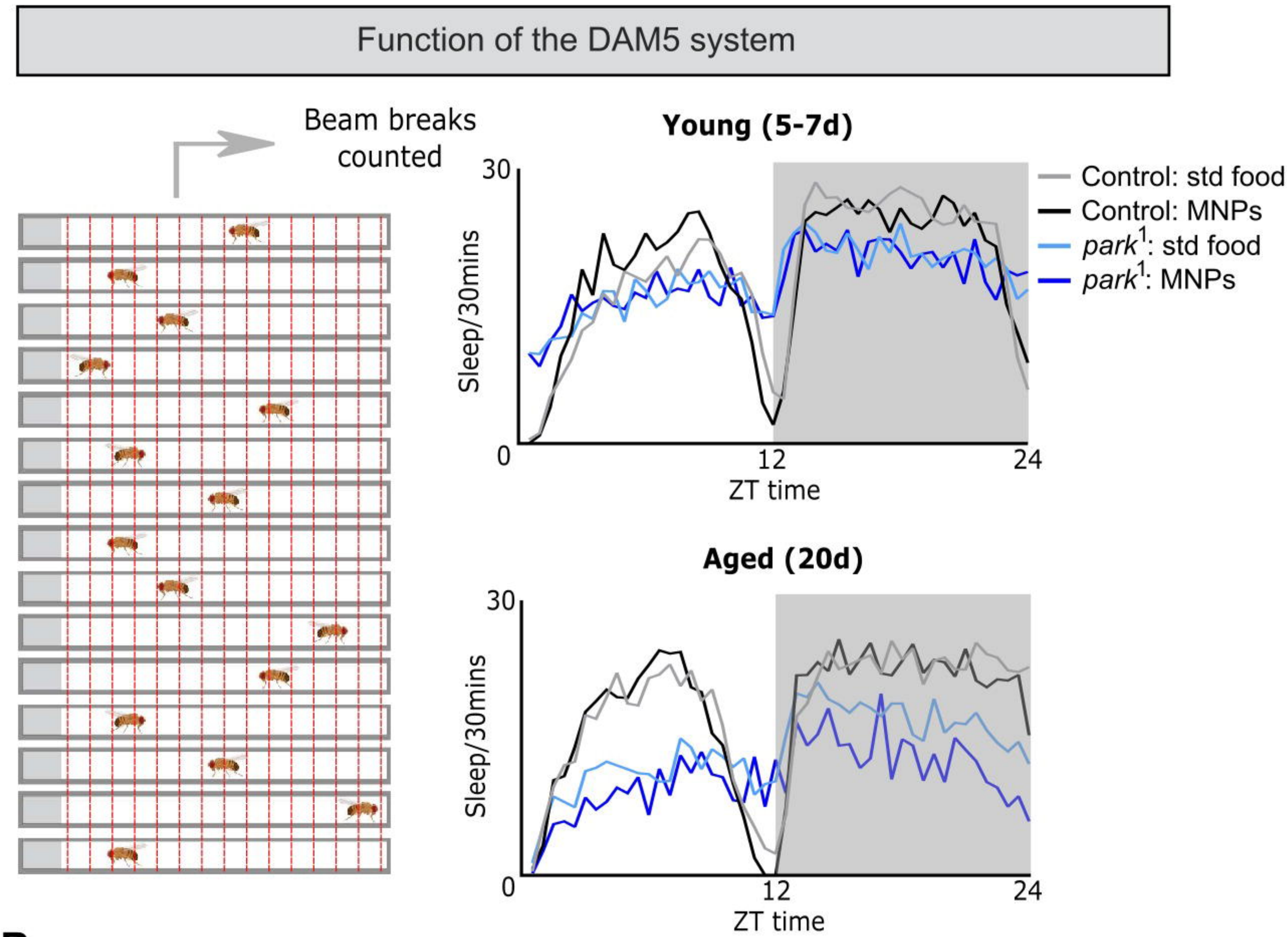
Function of the DAM5 system
Beam breaks counted
Young (5-7d)
Sleep/30mins
30
0
12
24
ZT time
Control: std food
Control: MNPs
park1: std food
park1: MNPs
Aged (20d)
Sleep/30mins
30
0
12
24
ZT time

B

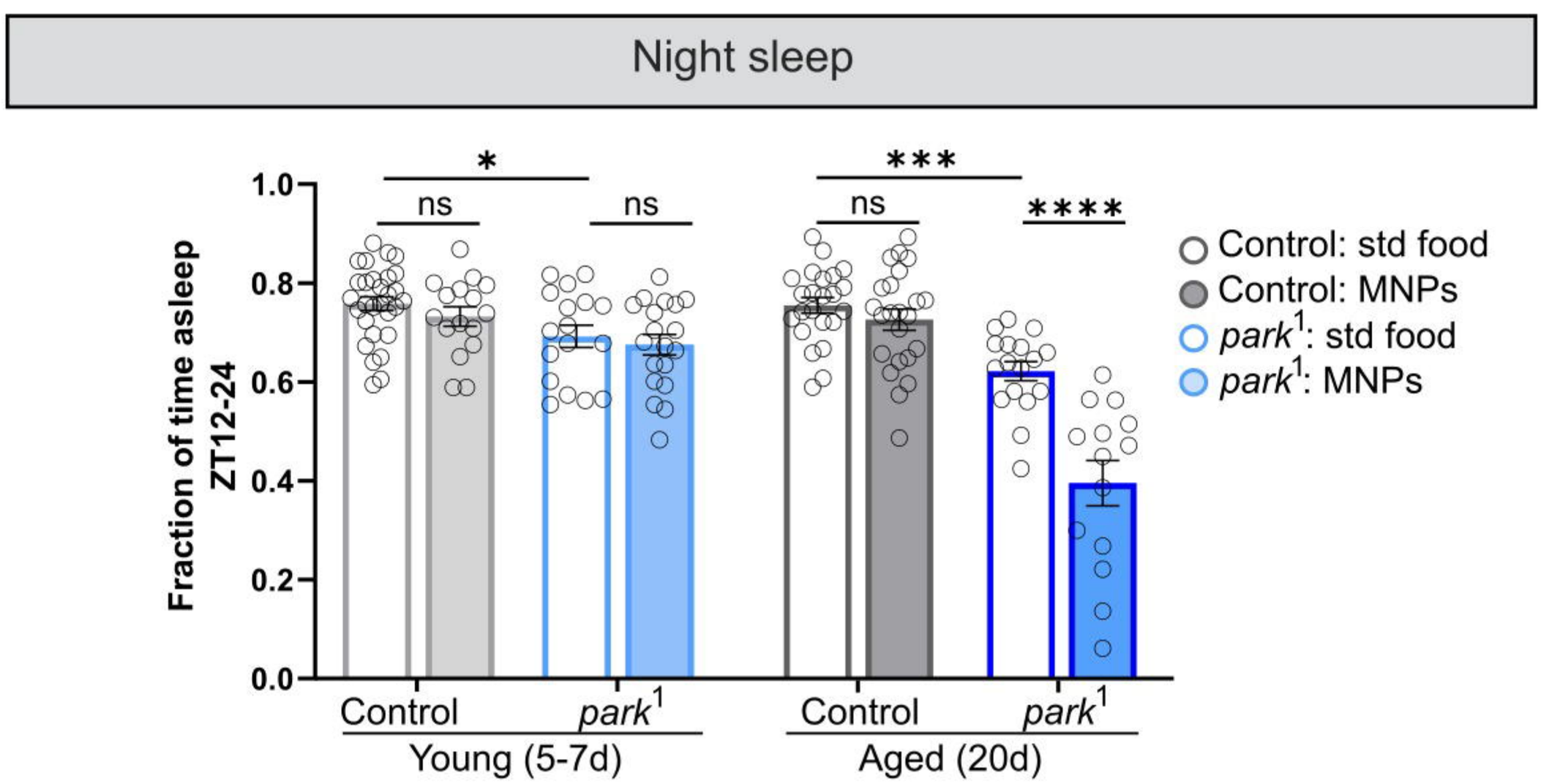
Night sleep
Fraction of time asleep ZT12-24
1.0
0.8
0.6
0.4
0.2
0.0
*
ns
ns
***
ns
****
Control
park1
Young (5-7d)
Control
park1
Aged (20d)
Control: std food
Control: MNPs
park1: std food
park1: MNPs